Struct Multidisc Optim (2014) 50:1103–1114
DOI 10.1007/s00158-014-1097-8

INDUSTRIAL APPLICATION

Optimal design of commercial vehicle systems using analytical target cascading

Namwoo Kang · Michael Kokkolaras · Panos Y. Papalambros · Seungwon Yoo · Wookjin Na · Jongchan Park · Dieter Featherman

Received: 1 October 2013 / Revised: 15 February 2014 / Accepted: 3 April 2014 / Published online: 7 August 2014

Abstract This paper presents an industrial application of the analytical target cascading methodology to optimal design of commercial vehicle systems. The design problems concern the suspension of a heavy-duty truck and the body structure of a small bus. The results provide valuable insights in the feasibility of system-level design targets and the adequacy of subproblem design spaces during product development.

Keywords Analytical target cascading · Optimal design · Vehicle systems

A previous version of this manuscript was presented at the 14th AIAA/ISSMO Multidisciplinary Analysis and Optimization Conference (September 17-19, 2012, Indianapolis, Indiana).

N. Kang
Design Science, University of Michigan,
Ann Arbor, MI 48109, USA

M. Kokkolaras (✉)
Department of Mechanical Engineering,
McGill University, Montreal,
QC H3A 0C3, Canada
e-mail: michael.kokkolaras@mcgill.ca

P. Y. Papalambros
Department of Mechanical Engineering,
University of Michigan, Ann Arbor,
MI 48109, USA

S. Yoo · W. Na · J. Park
Hyundai Motor Company, Hwaseong-Si,
Gyeonggi-Do 445706, Korea

D. Featherman
Altair Engineering, Troy, MI 48083, USA

1 Introduction

Design optimization of complex engineering systems can often be accomplished only by decomposition. The system is partitioned into subsystems, the subsystems are partitioned into components, the components into parts, and so on. The outcome of this object-based partitioning process is a multilevel hierarchy of system elements. The corresponding hierarchical optimization problem is solved by an appropriate coordination strategy, which should ensure that the solutions of the original All-In-One (AIO) problem and that of the partitioned problem are the same. It is emphasized here that the authors do not advocate decomposition approaches for optimal system design problems that can be solved using an AIO approach. Decomposition approaches are useful for problems that must be or already are decomposed due to complexity reasons or because subproblems are distributed to different design teams which may not have access to the information, formulation or models of the other subproblems.

Partitioning and coordination are referred to as a decomposition strategy. Hierarchical decomposition strategies facilitate employing decentralized optimization approaches that aid systems engineers to identify interactions among elements at lower levels and to transfer this information to higher levels. This system design practice is also reflected in the organizational structure of engineering companies. Research and Development (R&D) center of Hyundai Motor Company (HMC) features a partitioned organization reflecting the complexity of the vehicle engineering system. HMC is developing a hierarchical computational platform for commercial vehicle design to account for subsystem interactions and to investigate the relation between system design targets and subsystem responses during product development. The objective is to be able to determine

appropriate targets for current and new product designs that optimize vehicle-level performance. Determining appropriate targets that satisfy marketing goals and engineering feasibility is a significant task at the early stages of new vehicle design because system engineers typically have to rely on previous model specifications. Design specifications obtained using this hierarchical computational platform will serve design engineers well at the detail design phase.

Analytical target cascading (ATC) is an effective model-based, hierarchical optimization methodology to identify and account for subsystem interactions, and to translate system-level design targets to subsystem specifications while achieving system-level consistency and optimality (Kim 2001). ATC has been applied successfully to design problems in automotive, aerospace, manufacturing and civil engineering, e.g., Kim et al. (2002, 2003a, b), Kokkolaras et al. (2004), Blouin et al. (2004), Choudhary et al. (2005), Allison et al. (2006), Li et al. (2008a), Kang et al. (2013). The ATC methodology has theoretical convergence properties under standard assumptions (Michelena et al. 2003); its numerical behavior has been investigated and improved in Lassiter et al. (2005), Tosserams et al. (2006), Li et al. (2008b), Han and Papalambros (2010), and Wang et al. (2013). Recent formulation improvements and extensions have enhanced its computational behavior and applicability to a large class of multi-disciplinary design optimization (MDO) problems (Tosserams et al. 2010).

The scope of this paper is to demonstrate the successful implementation of the ATC process for two HMC vehicle systems. The first application considers the suspension design of a heavy-duty truck. The objective of this study is to investigate whether ATC would yield reasonable results relative to the existing HMC design target values. The second application considers the body structure design of a bus. The goal is to design a new-segment, middle-size bus. For these two design problems, the academic partners undertook developing and implementing the appropriate ATC formulations for the vehicle systems, while the industry partners were responsible for providing simulation models and ascertaining the practical quality of the results. Since modeling and computation are tightly related for successful optimization, the partners worked closely and interacted frequently during the execution of this study.

The article is organized as follows. The ATC algorithm used in this study is reviewed briefly in Section 2. The analysis models, ATC formulations and obtained results for the two applications are described in Sections 3 and 4, respectively. Conclusions are drawn in Section 5.

2 Analytical target cascading

Given a system partitioning that is usually object-based, ATC operates by exploiting the hierarchical functional dependencies that exist among subsystems, components, parts, etc., collectively referred to as system elements. For each element at each level of the partitioning hierarchy, a design optimization problem is formulated and solved to (i) satisfy targets set by elements at the level above and (ii) dictate targets for the elements at the level below. Analysis or simulation models are used to compute element responses given element designs. In this manner, top-level system design targets are propagated down to design specifications for lower-level elements. The resulting responses are then rebalanced at higher levels by iteratively adjusting designs (and thus specifications) to achieve system consistency.

The information flow to and from subproblem P_{ij} corresponding to the j-th element at the i-th level is illustrated in Fig. 1.

The general subproblem P_{ij} is formulated as

$$
\begin{aligned}
\min_{\bar{\mathbf{x}}_{ij}} \quad & f_{ij}(\bar{\mathbf{x}}_{ij}) + \phi(\mathbf{c}) \\
\text{with respect to} \quad & \bar{\mathbf{x}}_{ij} = \left[\mathbf{x}_{ij}, \mathbf{r}_{ij}, \mathbf{t}_{(i+1)k_1}, \ldots, \mathbf{t}_{(i+1)k_{n_{c_{ij}}}}\right] \\
\text{subject to} \quad & \mathbf{g}_{ij}(\bar{\mathbf{x}}_{ij}) \leq \mathbf{0} \\
& \mathbf{h}_{ij}(\bar{\mathbf{x}}_{ij}) = \mathbf{0} \\
\text{where} \quad & \mathbf{c} = \left[(\mathbf{t}_{ij} - \mathbf{r}_{ij}), (\mathbf{t}_{(i+1)k_1} - \mathbf{r}_{(i+1)k_1}), \ldots, \right. \\
& \qquad \left. \left(\mathbf{t}_{(i+1)k_{n_{c_{ij}}}} - \mathbf{r}_{(i+1)k_{n_{c_{ij}}}}\right)\right] \\
& \mathbf{r}_{ij} = \mathbf{a}_{ij}\left(\mathbf{x}_{ij}, \mathbf{t}_{(i+1)k_1}, \ldots, \mathbf{t}_{(i+1)k_{n_{c_{ij}}}}\right) \\
& \phi(\mathbf{c}) = \mathbf{v}^T(\mathbf{c}) + \|\mathbf{w} \circ \mathbf{c}\|_2^2 \ ,
\end{aligned}
\tag{1}
$$

where f_{ij} is the local objective function, $\bar{\mathbf{x}}_{ij}$ is the vector of optimization variables, $\mathbf{x}_{ij}$ is the vector of local design variables, $\mathbf{g}_{ij}$ and $\mathbf{h}_{ij}$ are the local inequality and equality design constraints, respectively, $\mathbf{t}_{ij}$ is the vector of children target optimization variables, $\mathbf{r}_{ij}$ is the vector of local element responses, $n_{c_{ij}}$ is the number of children, $\mathbf{c}$ is the vector of inconsistencies between targets and responses and ϕ is a penalty function. We use the augmented Lagrangian penalty function formulation reported in Tosserams et al. (2006), where $\mathbf{v}$ is the vector of Lagrange multipliers, $\mathbf{w}$ is the vector of quadratic penalty weights and the symbol $\circ$ denotes the Hadamard vector product (term-by-term multiplication of vectors).

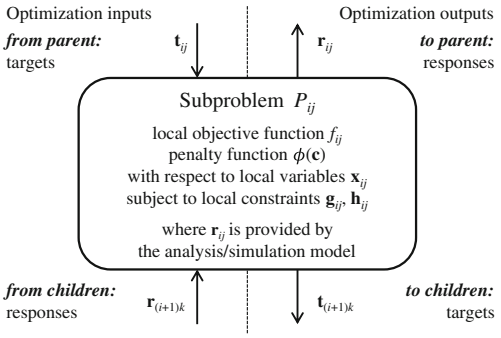

Fig. 1 Information flow for ATC subproblem (adapted from Tosserams et al. 2006)

We use the alternating directions scheme for updating the Lagrange multiplier estimates and the quadratic penalty weights after each ATC iteration as reported in Tosserams et al. (2006): after solving all subproblems of iteration k, the penalty weights are updated using

$$\mathbf{w}^{k+1} = \beta \mathbf{w}^k, \tag{2}$$

where $\beta \geq 1$ (in general, it is recommended that $2 < \beta < 3$). The Lagrange multiplier estimates are updated using

$$\mathbf{v}^{k+1} = \mathbf{v}^k + 2\,\mathbf{w}^k \circ \mathbf{w}^k \circ \mathbf{c}^k. \tag{3}$$

The convergence rate of the iterative ATC process varies from application to application as it depends highly on the coupling strength among the subproblems and the size of the feasible design space of each subproblem. We consider two termination criteria. The first criterion requires that the relative change in the values of the design optimization variables after 2 consecutive ATC iterations is smaller than a user-specified small positive threshold ε_1:

$$\frac{\|\mathbf{x}^k - \mathbf{x}^{k-1}\|_2}{\|\mathbf{x}^{k-1}\|_2} < \varepsilon_1. \tag{4}$$

The second criterion requires that the maximum relative consistency constraint violation is smaller than a user-specified small positive threshold ε_2

$$\max\left[\frac{t_1 - r_1}{t_1}, \frac{t_2 - r_2}{t_2}, \ldots, \frac{t_N - r_N}{t_N}\right]^k < \varepsilon_2, \tag{5}$$

where N is the total (cumulative) number of consistency constraints of the ATC problem and none of the targets is zero.

3 Heavy-duty truck suspension design

3.1 Problem formulation

The suspension system of heavy-duty trucks influences the static and dynamic loading applied to the road by the tires of the vehicle. This loading can cause significant damage to roads and bridges. For this reason, the Korean government regulates the axle load of heavy-duty trucks by requiring it to be less than 10,000 kg. In this study, the suspension of the HMC 8x4 25.5T dump truck is designed to conform to this axle-load regulation. The objective is to find optimal suspension characteristics (e.g., stiffness) for the 3 suspensions of the vehicle so that the axle load is as close as possible to 10,000 kg for each of the 4 vehicle axles. According to the existing design of an 8x4 25.5T dump truck shown in Fig. 2, each of the two front suspensions supports one of the front two axles.

The two rear axles share one suspension system. All suspensions consist of leaf springs. The helper spring is engaged in heavy payload cases to support the rear suspension system. This enables the rear suspension system to have a lower stiffness so that ride comfort is improved in light payload cases. The free camber denotes the vertical distance between the 2nd front axle and all other axles. This allows the 2nd front axle to be loaded faster and more than the other axles.

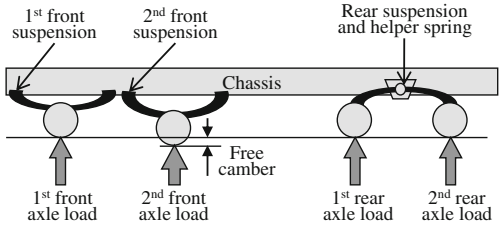

Fig. 2 Schematic of current suspension system of HMC 8x4 heavy-duty dump truck

The ATC decomposition for the axle-load problem consists of two levels and is shown schematically in Fig. 3. The system level represents the truck's chassis and the subsystem level includes the suspensions. The responses, linking variables (target-response pairs), local design variables and parameters of the ATC formulation are listed in Table 1.

The system-level problem is formulated as

$$\begin{aligned}
\min_{\bar{\mathbf{x}}} \quad & \|\tfrac{\mathbf{RF}}{10000} - \mathbf{1}\|_2^2 + \phi(\mathbf{c}) \\
\text{with respect to} \quad & \bar{\mathbf{x}} = \left[CB,\, D_h,\, K_h,\, K_{f_1}^U,\, K_{f_2}^U,\, K_r^U\right] \\
\text{subject to} \quad & lb \leq \bar{\mathbf{x}} \leq ub \\
& RF_i - 10000 \leq \varepsilon \\
\text{where} \quad & RF_i = Radioss(\bar{\mathbf{x}},\, K_{ft},\, K_{rt}),\ i = 1, 2, 3, 4 \\
& \mathbf{c} = \left[\tfrac{K_{f_1}^U - K_{f_1}^L}{K_{f_1}^U},\, \tfrac{K_{f_2}^U - K_{f_2}^L}{K_{f_2}^U},\, \tfrac{K_r^U - K_r^L}{K_r^U}\right]
\end{aligned} \tag{6}$$

RF is the vector of axle loads. The local design variables include the relative free camber CB of the 2nd front suspension, the gap D_h between the chassis and the helper spring at zero load, and the helper spring stiffness K_h. The linking variables between the system and subsystem levels are the stiffness of the 1st front suspension, the 2nd front suspension and the rear suspension (K_{f_1}, K_{f_2} and K_r, respectively). Superscripts $(\cdot)^U$ and $(\cdot)^L$ indicate upper and lower level variables, respectively. Lower and upper bounds of local and linking design variables were determined based on values used currently by HMC. Tolerance constraints for exceeding RF_i design targets are included according to regulations.

We used Matlab as the computational platform for implementing the ATC process and integrating the analysis tools, making system calls to the required simulations either directly or through Matlab's optimization toolbox[1].

[1] This is the case for both design examples and all levels presented in this paper.

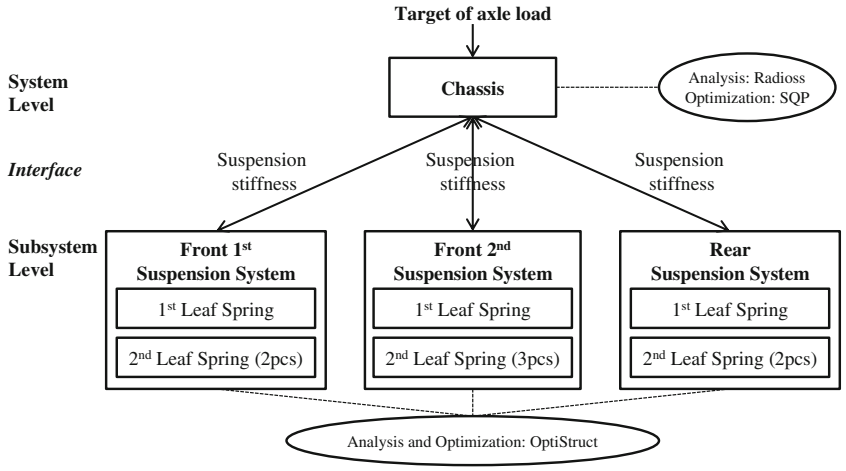

Fig. 3 Partitioning and information flow of the ATC process for the suspension problem

Axle loads are obtained by means of simulation models built using the Radioss software package of Altair Engineering (Altair 2012b). Matlab's implementation of the Sequential Quadratic Programming (SQP) algorithm (`fmincon`) is used for optimization (MathWorks 2012).

Axle loads are obtained by means of simulation models built using the Radioss software package of Altair Engineering (Altair 2012b). Matlab's implementation of the Sequential Quadratic Programming (SQP) algorithm (`fmincon`) is used for optimization (MathWorks 2012).

At the subsystem level, the 1st front and rear suspensions consist of three leaf springs. The 2nd front suspension consists of four leaf springs. Note that for all suspensions, the design of the first, large leaf spring differs from that of the other leaf springs, which are all identical. To satisfy the target values obtained at the system level, the ATC subproblem for each suspension j, where $j \in \{f_1, f_2, r\}$, is given by

$$\begin{aligned} \min_{\mathbf{x}_j} \quad & \phi(c) \\ \text{with respect to} \quad & \mathbf{x}_j = [A_{jk}, B_{jk}, C_{jk}, D_{jk}, L_{3jk}],\ k = 1, 2 \\ \text{subject to} \quad & lb \le \mathbf{x}_j \le ub \\ & \sigma_{max_j} \le ub \\ \text{where} \quad & \left[K_j^L, \sigma_{max_j}\right] \\ & \quad = OptiStruct(\mathbf{x}_j, L_1, L_2, L_4, L_5, L_6) \\ & c = \frac{K_j^U - K_j^L}{K_j^U} \end{aligned} \tag{7}$$

Table 1 Responses, variables and parameters for axle-load problem

Level	Variables and parameters
System level	**Responses**
	RF_i: i-th axle load (i = 1, 2, 3, 4)
	Local design variables
	K_h: Helper spring stiffness
	D_h: Gap between chassis and helper spring
	CB: Relative free camber of front 2nd suspension
	Parameters
	K_{ft}: Front tire stiffness
	K_{rt}: Rear tire stiffness
Interface	**Linking variables between system level and subsystem level**
	K_j: Stiffness of suspension j
	($j \in \{f_1$: 1st front, f_2: 2nd front, r: rear$\}$)
Subsystem level	**Local design variables**
	$A_{jk}B_{jk}C_{jk}D_{jk}L_{3jk}$: Dimensions of k-th leaf spring in suspension j ($j \in \{f_1, f_2, r\}$)(k = 1, 2)
	Parameters
	$L_1L_2L_4L_5L_6$: Fixed dimensions of leaf spring

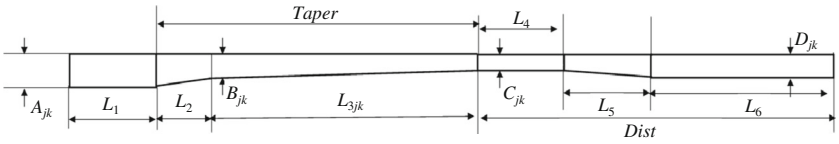

Fig. 4 OptiStruct model of suspension system and associated design variables and parameters

The local design variables A_{jk}, B_{jk}, C_{jk}, D_{jk}, L_{3jk} are the cross section dimensions of the k-th leaf spring of suspension j. Dimensions L_1, L_2, L_4, L_5, L_6 are fixed parameters in all springs. Since leaf springs are designed in symmetry, dimensions of only half spring model are considered as shown in Fig. 4.

The lower and upper bounds of local design variables were defined based on the leaf spring design space currently explored at HMC. The stiffness K_j and maximum stress σ_{max_j} of suspension j are calculated by means of simulation models built using the OptiStruct software package of Altair Engineering (Altair 2012a). Note that OptiStruct is used both for analysis and optimization by implementing the ATC subproblem formulation directly into the simulation model. This is a novel implementation feature of the ATC methodology.

3.2 Results

Using $\beta = 1.25$ and $\varepsilon_1 = \varepsilon_2 = 0.01$ (i.e., 1 %), the ATC process converged after 2 iterations.[2] The obtained target values for the responses are listed in Table 2.

The results demonstrate that there is a tradeoff between the front and rear axles: For the given problem formulation, design space and simulation models, minimizing the deviation of the front and rear axle loads from the regulation target values are competing objectives. Essentially, the squared L_2 norm term in the objective function of problem (6) represents an aggregate function of four competing objectives. Thus, we report the decrease of this aggregate value to demonstrate the optimization benefit. Note that it is left to the design engineer's discretion to solve the problem for different weights on the four targets if they wish to emphasize some axle(s) over the others and generate Pareto sets. This exercise is beyond the scope of this paper.

Table 3 reports optimal values for the target-response pairs.

[2]On an Intel i7 CPU 860@2.80GHz and 8.00GB RAM, one system-level function evaluation (i.e., Radioss simulation) takes 5 seconds on average, and the subproblem solution required 40 function evaluations on average; at the subsystem level, one Optistruct problem solution required 20 seconds on average. Consequently, one ATC iteration requires roughly 4 minutes.

Table 4 reports optimal values of local design variables at the system level. It can be seen that the optimal value of the relative free camber of the 2nd front suspension is quite different from the baseline value. This is because it contributes most to the response improvement of the 2nd front axle load (see Table 2).

Table 5 reports optimal design variables of leaf springs for each suspension.

The design variables reflect deviation from baseline leaf spring dimension values as follows: new dimension value = baseline value + design variable × increment parameter value, where the increment parameter value was selected by HMC designers. Superscripts $(\cdot)^{lb}$ and $(\cdot)^{ub}$ indicate optimal values hitting lower or upper bounds, respectively. Five dimensions of the 2nd front suspension are hitting their lower bounds, which indicates that the design space may be over-restricted; a parametric study with respect to these variable bounds is recommended.

In Fig. 5, we present the convergence history of the two termination criteria for 10 ATC iterations to obtain an enhanced understanding of the behavior of this problem. We can observe that if the desired maximum relative consistency constraint violation were 0.2 % (i.e., 0.002), then all 10 ATC iterations would have been necessary.

4 Bus body structure design

4.1 Problem formulation

Determining stiffness and mass design specifications for each body assembly is a challenging task for bus body structure designers. The objective of this bus body structure design study is to minimize mass of body structure and

Table 2 Baseline and optimal values for targets at the system level

Response	Target value	Baseline value	Optimal value
1st front axle load [kg]	10,000	10,549	10,199
2nd front axle load [kg]	10,000	9,578	10,130
1st rear axle load [kg]	10,000	9,956	9,856
2nd rear axle load [kg]	10,000	9,956	9,856
$\left\\| \frac{\mathbf{RF}}{\mathbf{10000}} - \mathbf{1} \right\\|_2^2$	–	4.83e-03	9.76e-04

Table 3 Target and response values for the linking variables between vehicle and system levels

Variable	Target value from system level	Response value from subsystem level	Deviation between target and response
1st front suspension stiffness [N/mm]	549.3	550.1	−0.1 %
2nd front suspension stiffness [N/mm]	551.1	551.6	−0.1 %
Rear suspension stiffness [N/mm]	2300.0	2290.3	0.4 %

Table 4 Baseline and optimal values for the local design variables computed at the system level

Variable	Baseline value	Optimal value
Gap between chassis and helper spring [mm]	17.50	18.58
Relative free camber of 2nd front suspension [mm]	0.00	7.57
Helper spring stiffness [N/mm]	1350	1350

Table 5 Optimal values for local design variables computed at the subsystem level

	1st front suspension		2nd front suspension		Rear suspension	
	1st spring	2nd spring	1st spring	2nd spring	1st spring	2nd spring
A	−7.92e−01	−7.94e−01	$-1.00e+00^{lb}$	$-3.00e+00^{lb}$	6.20e+00	6.20e+00
B	−3.46e−04	−2.20e−01	$-1.50e+00^{lb}$	$-1.50e+00^{lb}$	9.69e+00	9.70e+00
C	−4.46e−04	−5.16e−01	$-3.50e+00^{lb}$	−1.79e+00	1.23e+01	1.40e+01
D	−2.23e−05	−4.35e−05	−1.25e−19	−1.82e−19	9.99e+00	9.99e+00
L_3	−3.85e−06	−7.57e−06	−7.18e−22	7.06e−20	2.79e+01	8.84e+01

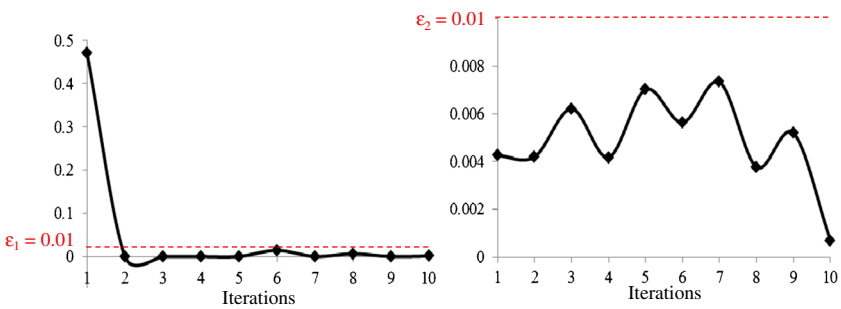

Fig. 5 Convergence history of ATC termination criteria for the suspension design problem

(a) First termination criterion (b) Second termination criterion

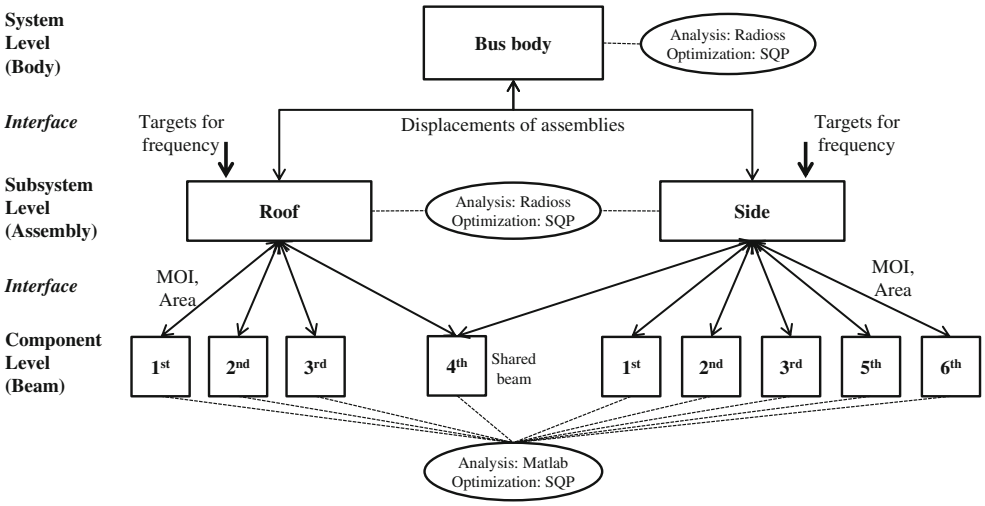

Fig. 6 Partitioning and information flow of the ATC process for the bus body structure problem

Table 6 Targets, responses, variables and parameters for the bus body structure problem

Level	Variables and parameters
System level	**Responses**
	M: Total mass
	f_k: Frequency of vehicle of k-th normal mode (k = 1, 2)
	Local design variables
	a_i: Proportionality factor of material property of i-th assembly
	(i = 1: roof, 2: side, 3: front, 4: rear, 5: floor)
	Parameters
	E_0: Initial modulus of elasticity of steel
	ρ_0: Initial density of steel
Interface	**Linking responses between system level and subsystem level**
	d_{bi}: Displacement of i-th assembly for bending (i = 1: roof, 2: side)
	d_{ti}: Displacement of i-th assembly for torsion (i = 1: roof, 2: side)
Subsystem level	**Local targets**
	f_{ki}^t: Target frequency of k-th normal mode for i-th assembly
	(k = 1, 2; i = 1: roof, 2: side)
	Responses
	M_i: Mass of i-th assembly (i=1: roof, 2: side)
	f_{ki}: Frequency of k-th normal mode for i-th assembly
	(k = 1, 2; i = 1: roof, 2: side)
Interface	**Linking responses between subsystem level and component level**
	$I_{1_{ij}}$: MOI in plane 1 for i-th assembly and j-th beam
	$I_{2_{ij}}$: MOI in plane 2 for i-th assembly and j-th beam
	A_{ij}: Area of cross section for i-th assembly and j-th beam
	(i = 1: roof; j = 1, 2, 3, 4) (i = 2: side; j = 1, 2, 3, 4, 5, 6)
Component level	**Local design variables**
	w_{ij}: Width of cross section for i-th assembly and j-th beam
	h_{ij}: Height of cross section for i-th assembly and j-th beam
	t_{ij}: Thickness of cross section for i-th assembly and j-th beam
	(i = 1: roof; j = 1, 2, 3, 4) (i = 2: side; j = 1, 2, 3, 4, 5, 6)

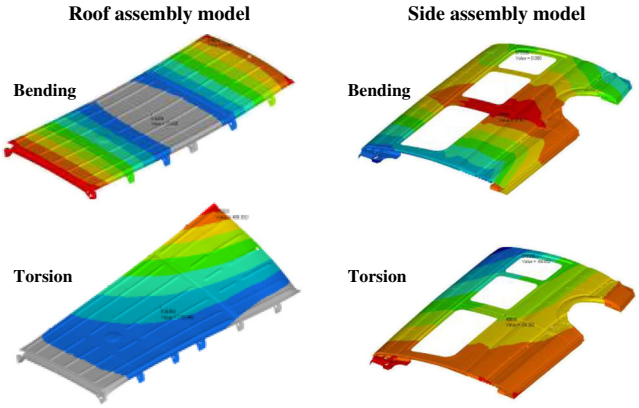

Fig. 7 Roof and side assemblies of the bus body structure under bending and torsion loading cases

find optimal structural stiffness of its assemblies by optimizing beam cross sections. Static and dynamic stiffness are considered in this study. Static stiffness is considered by means of assembly displacements. For each assembly, displacements are considered under bending and torsion deformation modes. For bending, a single force (1000 N) is applied at the center of each assembly. For torsion, a single force (500 N) is applied at a given node of each assembly. Dynamic stiffness is considered by means of normal mode frequencies. We assume that stress constraints are dominated by displacement constraints; they are thus not included in the optimization problem formulation. The ATC decomposition and information flow is depicted in Fig. 6.

The ATC hierarchy of the bus structure problem consists of three levels: a system level, a subsystem level and a component level. The system level represents the whole bus body structure, which consists of five assemblies (roof, side, front, rear and floor) modeled with beam elements. As depicted in Fig. 6, in this study we focus on the design of the roof and side assemblies. The nomenclature of the ATC formulation is presented in Table 6.

4.1.1 System-level problem

The system-level problem is formulated as

$$
\begin{array}{ll}
\min\limits_{\mathbf{x}} & \frac{M}{m} + \phi(\mathbf{c}) \\
\text{with respect to} & \mathbf{x} = [a_1, a_2, a_3, a_4, a_5] \\
\text{subject to} & lb \le \mathbf{x} \le ub \\
 & lb \le \mathbf{f} \\
\text{where} & [M, \mathbf{f}, \mathbf{d}^U] = Radioss(\mathbf{x}, E_0, \rho_0) \\
 & \mathbf{f} = [f_1, f_2] \\
 & \mathbf{d}^U = [d_{b1}^U, d_{t1}^U, d_{b2}^U, d_{t2}^U] \\
 & \mathbf{c} = \frac{\mathbf{d}^U - \mathbf{d}^L}{\mathbf{d}^U} \quad \text{(component by component division)}
\end{array}
\tag{8}
$$

The objective is to minimize total mass of the bus body M (we use a baseline mass m to scale this term of the objective function). The local design variables are material properties that affect static stiffness; a_i indicate proportionality factors of the material properties of the five assemblies, that change the modulus of elasticity and density (i.e., optimal modulus of elasticity = optimal value of a_i × initial modulus of elasticity E_0 and optimal density = optimal value of a_i × initial density ρ_0). The initial material properties are E_0 = 210 GPa and ρ_0 = 7850 kg/m^3 (steel). Subassembly displacements are used as linking variables between the system level and the subsystem level; d_{b1} and d_{t1} indicate roof assembly displacements corresponding to bending and torsion load cases, respectively; d_{b2} and d_{t2} indicate side assembly displacements for bending and torsion load cases, respectively. Superscripts $(\cdot)^U$ and $(\cdot)^L$ denote values computed at the system (upper) and subsystem (lower) levels, respectively. Frequencies have only lower bounds; f_1 denotes 1st normal mode frequency and f_2 denotes 2nd normal mode frequency. All responses are obtained by means of simulation models built using Radioss. Matlab's implementation of the SQP algorithm was used for optimization.

Table 7 Baseline and optimal values for target at the system and subsystem level

Level	Response	Target value	Baseline value	Optimal value
System	Total mass, M [kg]	0	5,803	4,472
Sub-system	Mass of roof, M_1 [kg]	0	416	467
	Mass of side, M_2 [kg]	0	871	980
	1st mode frequency of roof, f_{11} [Hz]	5.825	5.236	4.846
	2nd mode frequency of roof, f_{21} [Hz]	8.650	9.052	8.832
	1st mode frequency of side, f_{12} [Hz]	5.676	10.008	8.631
	2nd mode frequency of side, f_{22} [Hz]	7.785	12.879	12.834
	$\lVert \frac{\mathbf{f}' - \mathbf{f}}{\mathbf{f}'} \rVert_2^2$	–	1.023	0.720

Table 8 Target and response values for linking variables between system and subsystem levels

Variable	Target value from system level	Response value from subsystem level	Deviation between target and response
Displacement of roof for bending, d_{b1} [mm]	66.9	67.4	−0.8 %
Displacement of roof for torsion, d_{t1} [mm]	451.5	447.9	0.8 %
Displacement of side for bending, d_{b2} [mm]	17.7	19.7	−11.4 %
Displacement of side for torsion, d_{t2} [mm]	85.7	77.3	9.9 %

4.1.2 Subsystem-level problem

The subsystem level considers two assemblies (roof and side), as they are the most important contributors to the stiffness of the bus body structure; they are depicted in Fig. 7.

The two ATC subproblems of roof and side assemblies are formulated similarly; only the roof subproblem is thus formulated here for brevity.

$$
\begin{aligned}
\min_{\mathbf{I}_1^U, \mathbf{I}_2^U, \mathbf{A}^U} \quad & \tfrac{M_1}{m_1} + \| \tfrac{\mathbf{f}_1^t - \mathbf{f}_1}{\mathbf{f}_1^t} \|_2^2 + \phi(\mathbf{c}) \\
\text{subject to} \quad & lb \le \mathbf{I}_1^U \le ub \\
& lb \le \mathbf{I}_2^U \le ub \\
& lb \le \mathbf{A}^U \le ub \\
\text{where} \quad & [M_1, \mathbf{f}_1, \mathbf{d}^L] = Radioss\left(\mathbf{I}_1^U, \mathbf{I}_2^U, \mathbf{A}^U\right) \\
& \mathbf{f}_1 = [f_{11}, f_{21}] \\
& \mathbf{d}^L = [d_{b1}^L, d_{t1}^L] \\
& \mathbf{I}_1^U = [I_{1_{11}}^U, I_{1_{12}}^U, I_{1_{13}}^U, I_{1_{14}}^U] \\
& \mathbf{I}_2^U = [I_{2_{11}}^U, I_{2_{12}}^U, I_{2_{13}}^U, I_{2_{14}}^U] \\
& \mathbf{A}^U = [A_{11}^U, A_{12}^U, A_{13}^U, A_{14}^U] \\
& \mathbf{c} = \left[\tfrac{\mathbf{d}^U - \mathbf{d}^L}{\mathbf{d}^U}, \tfrac{\mathbf{I}_1^U - \mathbf{I}_1^L}{\mathbf{I}_1^U}, \tfrac{\mathbf{I}_2^U - \mathbf{I}_2^L}{\mathbf{I}_2^U}, \tfrac{\mathbf{A}^U - \mathbf{A}^L}{\mathbf{A}^U} \right] \\
& \quad \text{(component by component division)}
\end{aligned}
\tag{9}
$$

The objective of the subsystem-level problem(s) is to minimize assembly mass and to satisfy local targets of normal mode frequencies. M_1 is the mass of roof assembly (m_1 is a baseline mass); $\mathbf{f}_1^t$ and $\mathbf{f}_1$ are the local frequency target and responses, respectively. The subsystem-level problem does not have any local design variables. The linking variables with the system level are the roof displacements for bending and torsion d_{b1} and d_{t1}, respectively. The linking variables with the component level are the beam cross section moments of inertia (MOI) of the four roof beams: $I_{1_{11}}, I_{1_{12}}, I_{1_{13}}, I_{1_{14}}$. $\mathbf{I}_2$ is the vector of MOI in plane 2, and $\mathbf{A}$ is the vector of area of four beam cross sections. Superscripts $(\cdot)^U$ and $(\cdot)^L$ denote values computed at the subsystem (upper) and component (lower) levels, respectively. All responses are obtained by means of Radioss simulation models. Matlab's implementation of the SQP algorithm was used for optimization.

4.1.3 Component-level problem

The component level includes the beam cross section models. The roof assembly has four beams and the side assembly has six beams. All beam ATC subproblems are formulated similarly; thus, we present here only the ATC subproblem for the 4th roof beam.

$$
\begin{aligned}
\min_{\mathbf{x}} \quad & \phi(\mathbf{c}) \\
\text{with respect to} \quad & \mathbf{x} = [w_{14}, h_{14}, t_{14}] \\
\text{subject to} \quad & lb \le \mathbf{x} \le ub \\
\text{where} \quad & \left[I_{1_{14}}^L, I_{2_{14}}^L, A_{14}^L \right] = Matlab(w_{14}, h_{14}, t_{14}) \\
& \mathbf{c} = \left[\tfrac{I_{1_{14}}^U - I_{1_{14}}^L}{I_{1_{14}}^U}, \tfrac{I_{2_{14}}^U - I_{2_{14}}^L}{I_{2_{14}}^U}, \tfrac{A_{14}^U - A_{14}^L}{A_{14}^U}, \right. \\
& \quad \left. \tfrac{I_{2_{24}}^U - I_{1_{14}}^L}{I_{2_{24}}^U}, \tfrac{I_{1_{24}}^U - I_{2_{14}}^L}{I_{1_{24}}^U}, \tfrac{A_{24}^U - A_{14}^L}{A_{24}^U} \right]
\end{aligned}
\tag{10}
$$

The objective function includes only the penalty function ϕ to minimize the deviation of the linking variables between the subsystem and component levels. The local design variables are the beam cross section dimensions w_{14}, h_{14} and t_{14} (width, height and thickness, respectively). The 4th beam of the roof assembly is shared with the side assembly (as shown in Fig. 6). Therefore, linking variable deviations are related with two parents: roof assembly $\left(\text{i.e.,} \left[\tfrac{I_{1_{14}}^U - I_{1_{14}}^L}{I_{1_{14}}^U}, \tfrac{I_{2_{14}}^U - I_{2_{14}}^L}{I_{2_{14}}^U}, \tfrac{A_{14}^U - A_{14}^L}{A_{14}^U} \right]\right)$ and side assembly $\left(\text{i.e.,} \left[\tfrac{I_{2_{24}}^U - I_{1_{14}}^L}{I_{2_{24}}^U}, \tfrac{I_{1_{24}}^U - I_{2_{14}}^L}{I_{1_{24}}^U}, \tfrac{A_{24}^U - A_{14}^L}{A_{24}^U} \right]\right)$. The roof

Table 9 Baseline and optimal values for local design variables computed at the system level

Variable: Proportionality factor of material property of	Baseline value	Optimal value
roof, a_1	1.0000	1.0852
side, a_2	1.0000	0.9879
front, a_3	1.0000	0.5000^{lb}
rear, a_4	1.0000	1.3398
floor, a_5	1.0000	0.7816

Table 10 Target and response values for linking variables between subsystem and component levels

Assembly	Beam	Variable	Target value from subsystem level	Response value from component level	Deviation between target and response
Roof	1st	Area [mm^2], A_{11}	176	176	−0.2 %
		MOI$_1$ [mm^4], $I_{1_{11}}$	131575	131524	0.0 %
		MOI$_2$ [mm^4], $I_{2_{11}}$	46696	46689	0.0 %
	2nd	A_{12}	177	177	−0.1 %
		$I_{1_{12}}$	132550	132521	0.0 %
		$I_{2_{12}}$	49090	49085	0.0 %
	3rd	A_{13}	191	192	−0.2 %
		$I_{1_{13}}$	167037	166959	0.0 %
		$I_{2_{13}}$	61884	61873	0.0 %
	4th	A_{14}	396	390	1.4 %
		$I_{1_{14}}$	357251	376540	−5.4 %
		$I_{2_{14}}$	236816	256308	−8.2 %
Side	1st	A_{21}	221	221	0.0 %
		$I_{1_{21}}$	116928	117002	−0.1 %
		$I_{2_{21}}$	231381	231612	−0.1 %
	2nd	A_{22}	361	361	0.0 %
		$I_{1_{22}}$	123279	123277	0.0 %
		$I_{2_{22}}$	1403820	1403726	0.0 %
	3rd	A_{23}	400	400	0.0 %
		$I_{1_{23}}$	164087	163935	0.1 %
		$I_{2_{23}}$	1065583	1066092	0.0 %
	4th	A_{24}	392	390	0.5 %
		$I_{1_{24}}$	264417	256308	3.1 %
		$I_{2_{24}}$	556940	376540	32.4 %
	5th	A_{25}	187	188	−0.4 %
		$I_{1_{25}}$	32446	32439	0.0 %
		$I_{2_{25}}$	182475	182248	0.1 %
	6th	A_{26}	203	203	0.0 %
		$I_{1_{26}}$	90605	90603	0.0 %
		$I_{2_{26}}$	180106	180103	0.0 %

Table 11 Optimal values for local design variables computed at the component level

Assembly	Beam	Width, w_{ij} [mm]	Height, h_{ij} [mm]	Thickness, t_{ij} [mm]
Roof	1st	74.01	37.74	0.80^{lb}
	2nd	73.79	38.66	0.80^{lb}
	3rd	79.62	41.70	0.80
	4th	80.00^{ub}	62.24	1.40^{ub}
Side	1st	54.26	84.92	0.80^{lb}
	2nd	40.13	186.87	0.80^{lb}
	3rd	45.03	149.19	1.04
	4th	80.00^{ub}	62.24	1.40^{ub}
	5th	29.56	89.24	0.80^{lb}
	6th	49.92	78.30	0.80^{lb}

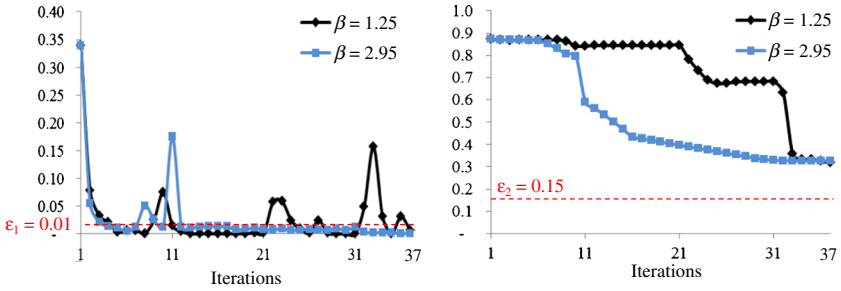

(a) First termination criterion (b) Second termination criterion

Fig. 8 Convergence history of ATC termination criteria for the bus design problem

and side models have opposite axis so that I_1 for roof and I_2 for side make a pair. Since this component has two parents, we use the non-hierarchical ATC formulation of Tosserams et al. (2010). According to this formulation, the 4th beam receives two targets (one from the roof assembly and one from the side assembly), and reports back one response to the two assemblies. All responses are calculated by means of analysis models implemented in Matlab. Matlab's implementation of the SQP algorithm was used for optimization.

4.2 Results

Using $\beta = 1.25$, $\varepsilon_1 = 0.01$ (i.e., 1 %) and $\varepsilon_2 = 0.15$ (i.e., 15 %), the ATC process did not manage to satisfy the maximum relative consistency constraint criterion after 37 iterations. Given the relatively high computational cost of the simulations,[3] we decided to halt the process and examine the results.

The target values for the responses computed at the system and subsystem levels are presented in Table 7.

In terms of total body structure mass, a significant improvement of 1,331 kg (22.9 %) over the baseline value has been achieved. The roof and side assembly masses M_1 and M_2 are larger than the basline because the former have to satisfy stiffness and frequency requirements, while the other assemblies are more flexible in their design having to satisfy only system-level requirements and constraints. Thus, the system-level design yields a smaller total mass M. Regarding the roof and side assembly 1st and 2nd mode frequencies, tradeoffs are identified, although they are not as intense as the axle load tradeoffs in the truck suspension design problem. Moreover, the mismatch is not significant in order to affect other component frequencies adversely. If the frequency at the subsystem level were treated as a local design constraint instead of a local objective, larger frequency values would be acceptable. We report here the decrease in the collective value of the squared L_2 norms used in the formulation of the subproblems (9) to demonstrate optimization benefits.

The response values at the subsystem level are reported in Table 8. They satisfy the target values from the system level with a maximum 15 % deviation ($\varepsilon_2 = 0.15$).

This can be considered reasonable given the stringent design constraints. Table 9 reports optimal values for local design variables at the system level.

Since material properties affect static stiffness directly, we observe that the rear assembly needs to be reinforced (optimal value for a_4 is larger than the baseline value). On the contrary, we can reduce the stiffness of the front and floor assemblies because (optimal values for a_3 and a_5 are lower than baseline values). Table 10 reports response values at the component level.

They satisfy the targets from the subsystem level reasonably well except for only one variable of the 4th side beam cross sections. The main reason is that the 4th side beam and the 4th roof beam are a shared component; thus, they are competing to satisfy two different targets, which is impossible in the given design space: the corresponding optimal values of the local design variables at the component level (listed in Table 11) are hitting their upper bounds. The beam configurations and/or the specifications of the design space need to be revisited. This exercise is out of the scope of this paper. Our objective is to illustrate how the ATC process can be used to help designers identify such issues.

Figure 8 illustrates the convergence history of the ATC process for the two termination criteria; we executed an additional ATC run with $\beta = 2.95$ to investigate whether the consistency constraint error would decrease faster. While this is indeed the case, the lowest value we could obtain was the same as for the $\beta = 1.25$ case.

However, the ATC process with $\beta = 2.95$ can be halted after about 15 iterations (i.e., one week) since the first termination criterion is satisfied and the value of the second termination criterion is not changing much. An examination

[3] On an Intel i7 CPU 860@2.80GHz and 8.00GB RAM, one system-level function evaluation (i.e., Radioss simulation) takes 7 minutes on average, and the subproblem solution required 50 function evaluations on average; at the subsystem level one function evaluation takes 12 seconds on average, and each of the two subproblems required 800 function evaluations on average; at the component level, computational cost is negligible. Consequently, one ATC iteration requires roughly half a day.

of the available results would also lead to the identification of the limited design space issue regarding the shared beam without having to spend another 20 iterations (or 10 days) of computations. An alternative to dealing with similar situations, where only 1 or 2 of tens of consistency constraints are exhibiting large deviations could be to average the maximum relative error. In this case, the violation would decrease from around 30 % to around 1 %.

5 Conclusion

The ATC methodology was applied to two commercial vehicle design problems with a significant number of variables, decomposition levels and modeling complexity. The obtained results are meaningful and demonstrate the value of ATC in an industry setting. An implementation novelty was that OptiStruct was used both for analysis and optimization for the subsystem-level subproblems of one design problem, making the ATC computational process more efficient.

For the suspension design problem of the heavy-duty truck, the objective was to bring the four vehicle axle loads as close as possible to the value of 10,000 kg. The optimal response values obtained using ATC are closer than baseline design values. The leaf spring design variable values satisfy stiffness targets required at the chassis level.

For the body structure design problem of the middle-size bus, the objective at the system level was to minimize the total mass. The optimal response value obtained using ATC is a significant improvement relative to baseline design.

In general, ATC results can provide useful insights and guidance regarding the feasibility of system-level design targets and the adequacy of subproblem and component design spaces. Using ATC results, design engineers can investigate whether attainable optimal values vary under different constraints, can obtain information on which subsystems and components affect system-level objectives and can gain insight on how subsystems and components should be modified to satisfy overall system design targets.

Acknowledgements The authors are grateful for the financial support of Hyundai Motor Company. Such support does not constitute an endorsement by the sponsor of the opinions expressed in this article.

References

Allison J, Walsh D, Kokkolaras M, Papalambros PY, Cartmell M (2006) Analytical target cascading in aircraft design. In: 44th AIAA Aerospace Sciences Meeting and Exhibit. Reno. AIAA-2006-1325

Altair (2012) OptiStruct Version 11.0, Available at: http://www.altairhyperworks.com

Altair (2012) Radioss Version 11.0, Available at: http://www.altairhyperworks.com

Blouin VY, Samuels HB, Fadel GM, Haque IU, Wagner JR (2004) Continuously variable transmission design for optimum vehicle performance by analytical target cascading. Int J Heavy Veh Syst 11(3–4):327–348

Choudhary R, Malkawi A, Papalambros PY (2005) Analytic target cascading in simulation-based building design. Autom Constr 14(4):551–568

Han J, Papalambros PY (2010) A note on the convergence of analytical target cascading with infinite norms. ASME J Mech Des 132(3):034502 1–6

Kang N, Kokkolaras M, Papalambros PY (2013) Solving multiobjective optimization problem using quasi-separable MDO formulations and analytic target cascading. In: 10th World Congress on Structural and Multidisciplinary Optimization. Orlando

Kim HM (2001) Target cascading in optimal system design, Ph.D. Dissertation, Mechanical Engineering Dept., University of Michigan, Ann Arbor, MI

Kim HM, Kokkolaras M, Louca LS, Delagrammatikas GJ, Michelena NF, Filipi ZS, Papalambros PY, Stein JL, Assanis DN (2002) Target cascading in vehicle redesign: a class VI truck study. Int J Veh Des 29(3):199–225

Kim HM, Michelena NF, Papalambros PY, Jiang T (2003a) Target cascading in optimal system design. ASME J Mech Des 125(3):474–480

Kim HM, Rideout DG, Papalambros PY, Stein JL (2003b) Analytical target cascading in automotive vehicle design. ASME J Mech Des 125:481–489

Kokkolaras M, Louca LS, Delagrammatikas GJ, Michelena NF, Filipi ZS, Papalambros PY, Stein JL, Assanis DN (2004) Simulation-based optimal design of heavy trucks by model-based decomposition: an extensive analytical target cascading case study. Int J Heavy Veh Syst 11(3-4):403–433

Lassiter JB, Wiecek MM, Andrighetti KR (2005) Lagrangian coordination and analytical target cascading: solving ATC-decomposed problems with Lagrangian duality. Optim Eng 6(3): 361381

Li Z, Kokkolaras M, Papalambros P, Hu SJ (2008a) Product and process tolerance allocation in multi-station compliant assembly using analytical target cascading. ASME J Mech Des 130(9):091701 1–9

Li Y., Lu Z., Michalek J. J. (2008b) Diagonal quadratic approximation for parallelization of analytical target cascading. ASME J Mech Des 130(5):051402 111

MathWorks (2012) Matlab R2012a, Available at: http://www.mathworks.com

Michelena N, Park H, Papalambros PY (2003) Convergence properties of analytical target cascading. AIAA J 41(5):897–905

Tosserams S, Etman LFP, Papalambros PY, Rooda JE (2006) An augmented Lagrangian relaxation for analytical target cascading using the alternating directions method of multipliers. Struct Multidiscip Optim 31(3):176–189

Tosserams S, Kokkolaras M, Etman LFP, Rooda JE (2010) A nonhierarchical formulation of analytical target cascading. ASME J Mech Des 132:051002 1–12

Wang W, Blouin VY, Gardenghi MK, Fadel GM, Wiecek MM, Sloop BC (2013) Cutting plane methods for analytical target cascading with augmented Lagrangian coordination. ASME J Mech Desi 135(10):104502 1–6